Pre-conference Field Trip

Ductile deformation and rheology of sub-continental mantle in hot collisional orogen: example from the folded Mohelno peridotite body and surrounding felsic granulites and metagabbros.

1. Introduction

The Bohemian Massif represents the easternmost exposure of the European Variscan belt (Fig. 1; (Edel and Weber, 1995; Franke, 2000). The present day structure of the Bohemian Massif originated by southeastward subduction of the Paleotethys Ordovician Ocean underneath the continental lithosphere during Upper Devonian. Closure of the Paleotethys Ocean followed by underthrusting the Saxothuringian continental crust led to development of double-thickened orogenic root represented by the Tepla-Barrandian and Moldanubian zones at Lower Carboniferous (e.g. (Schulmann et al., 2009). An opposite indentation of foreland continental Brunia promontory follows the thickening of the orogenic root domain that triggered extrusion and exhumation of the orogenic lower crust into the mid-crustal depths (Schulmann et al., 2005). The visited area is located in the Gföhl Unit representing outcrops of the orogenic lower crust at the eastern margin of the Bohemian massif (Fig. 2b).

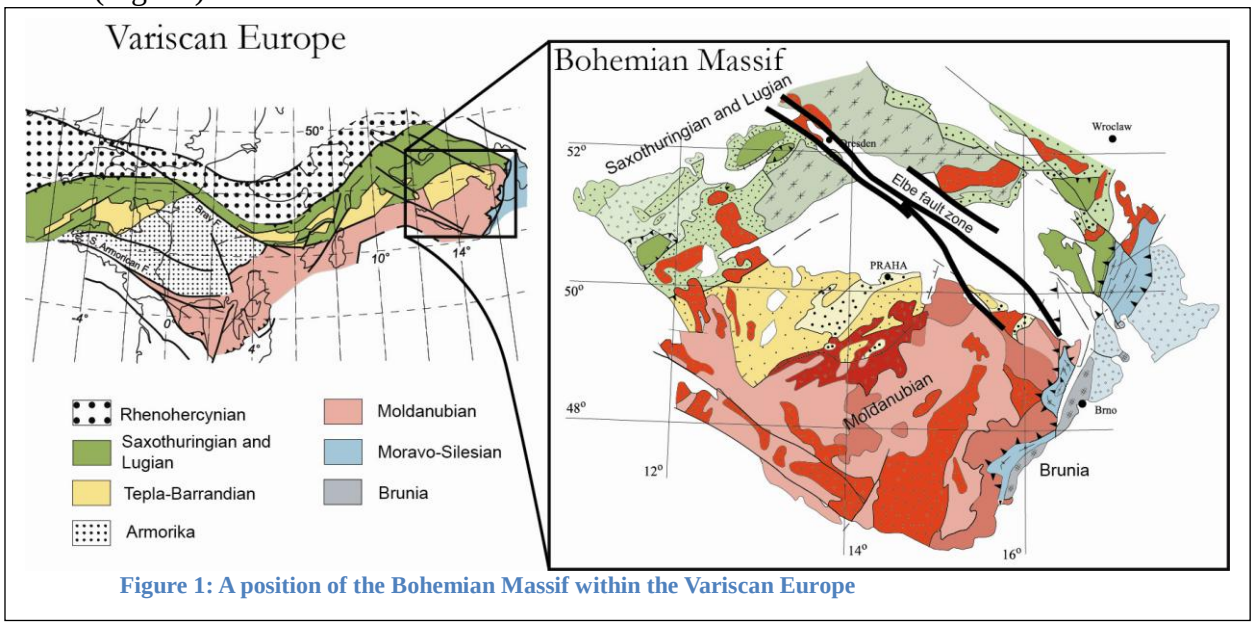

Figure 1: A position of the Bohemian Massif within the Variscan Europe

The Gföhl Unit consists of partially molten orthogneisses, amphibolites and migmatite gneisses including bodies of granulites, eclogites and peridotites (Tollmann, 1982). Felsic granulites of granite/rhyolite affinity (Fiala et al., 1987) are composed of quartz, garnet, kyanite, alkaline feldspar, plagioclase and rutile representing peak mineral assemblage (Carswell and O'Brien, 1993). Typical felsic granulites are interpreted as metamorphosed equivalents of Lower Palaeozoic, probably high-level granites buried to continental root during the Variscan collision (Janoušek et al., 2004; Janoušek and Holub, 2007; Lexa et al., 2011). Petrological studies of felsic and pyroxene bearing intermediate granulites show peak conditions of 800 – 1000°C and 16 – 20 kbar (Cooke, 2000; Cooke and O'Brien, 2001; Racek et al., 2006; Racek et al., 2008; Tajčmanová et al., 2006; Štípská et al., 2004) and amphibolites facies retrogression at 750 – 700°C and 9 – 4 kbar (Fig. 3). The process of vertical movement of high-grade granulites complexes to mid crustal levels has been recently described and attributed to a vertical extrusion of orogenic lower crust (Schulmann et al.,

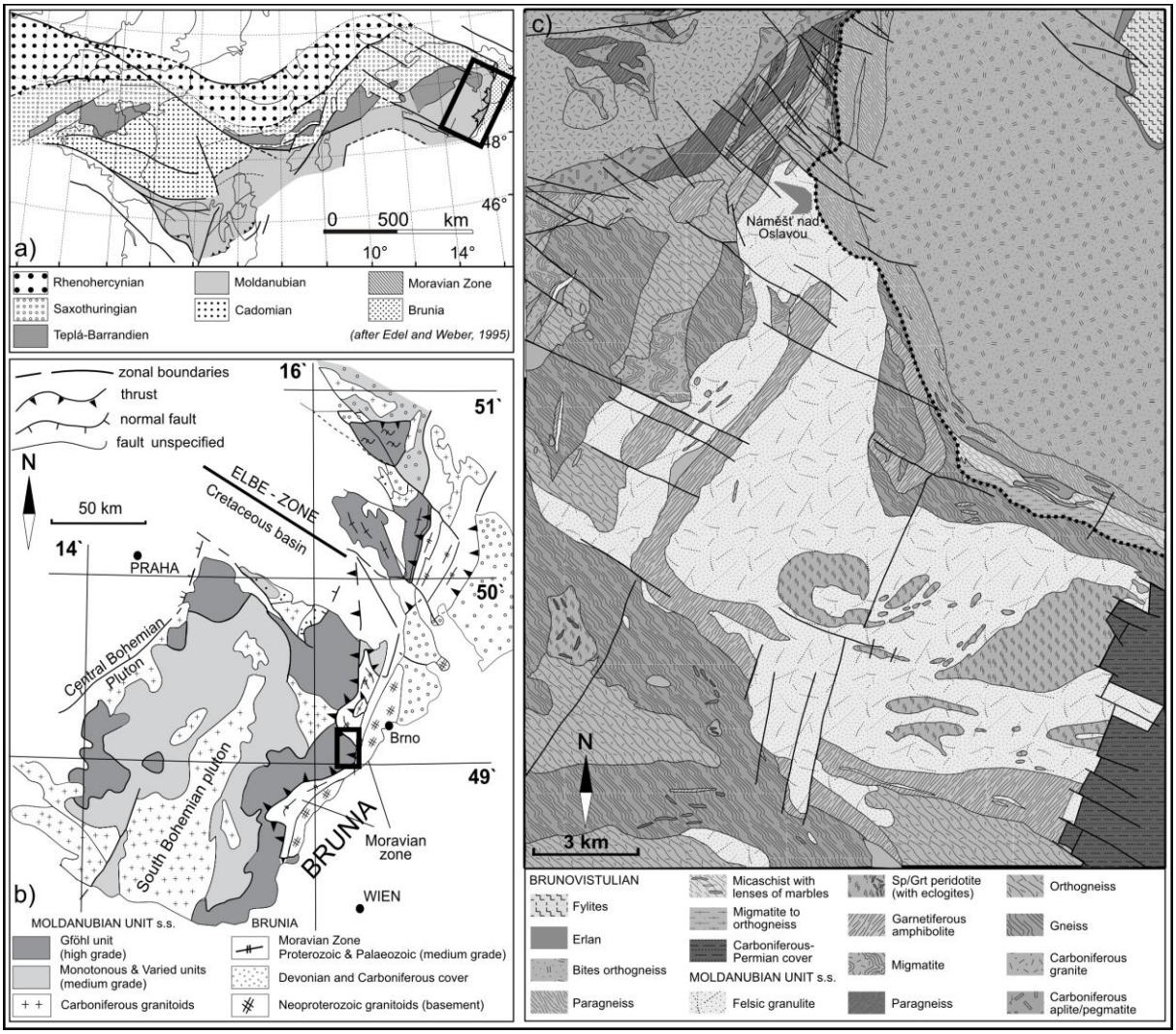

Figure 2: Geological setting: a) a position of the Bohemian Massif in the framework of the European Variscides (modified after Franke (2000)) and b) simplified tectonic map of the eastern margin of the Bohemian massif; c) a simplified geological map of the studied area according to the geological map 1:50000, sheet of the Czech Geological Survey.

2005; Schulmann et al., 2008; Tajčmanová et al., 2006). The extrusion was later followed by horizontal channel flow (Schulmann et al., 2008; Štípská et al., 2008) in middle crustal level, coupled with retrogression of granulites and amphibolites and intense melting (Hasalová et al., 2008a).

The studied granulite-peridotite rock association occurs within the Náměšť Granulite Massif (NGM) at the boundary with continental Brunia promontory to the east (Fig. 2b, c). The granulite body is nearly completely enveloped by a belt of pyroxene and/or garnet amphibolites with a tholeiitic geochemical signature (Šichtařová, 1981). This granulite-amphibolite complex is further surrounded by heterogenous gneisses ("the Gföhl gneisses") varying from migmatitic orthogneiss marked by qtz-kfs-plg-bt±grt±sill±ky mineral assemblage (Matějovská, 1975). Hasalová et al. (2008a,b) shown that different Gföhl gneiss types can be considered as continuous sequence ranging from banded orthogneiss to nebulitic migmatites, developed by melt infiltration in crustal channel.

The Mohelno peridotite belongs to numerous bodies of spinel to garnet peridotites enclosed within retrogressed granulite of the NGM. These bodies form lenses ranging from meters to several kilometers in size (Urban, 1992), while the Mohelno serpentinized peridotite exhibits a form of a large fold arc with decreasing thickness from ~1000m in the northern limb to ~300m in the southern one (Fig. 2c). Peridotites are strongly serpentinized (50-100%) but their original pristine microstructure is occasionally preserved. The original

mineral assemblage of peridotites is represented by olivine, orthopyroxene, clinopyroxene and spinel (Fig. 3, Stage IA, IB of Medaris et al. (1990)). Primary spinel is overgrown by garnet (Stage II) followed by further breakdown to clinopyroxene and spinel (Stage III) and amphibole and spinel symplectites (Stage IV) associated with fine grained mylonitic microstructure. Peridotites provide the geochemical signature characteristic for an asthenospheric origin, and because of presence of pyroxenite veins, it was proposed that original spinel peridotite developed at temperatures close to dry pyrolite solidus (Kamei et al., 2010; Medaris et al., 1990). However, pressure estimates for this evolutionary stage remain not quantified. According to standard geothermobarometry the peak mineral assemblage of garnet peridotite occurred at 2.3–2.8GPa and temperature ~1200ºC (Medaris et al., 1990) or at 1.8-2.5GPa at 1100-1250ºC (Kamei et al., 2010) while mylonitic microstructure with secondary spinel reveals conditions of 0.8-1.5GPa at 800-950ºC (Fig. 3). The clinopyroxene-spinel and amphibole-spinel kelyphite assemblage around garnets are correlated with granulite facies and amphibolite facies retrogression in surrounding granulites, respectively (Kamei et al., 2010; Medaris et al., 2005; Medaris et al., 1990). The contact zone between granulite and peridotite along the inner margin of the Mohelno peridotite body is characterized by presence of various magmatic rocks as hornblendite, biotitite and gabbrodiorite interpreted as reaction zone (Dobretsov et al., 1984).

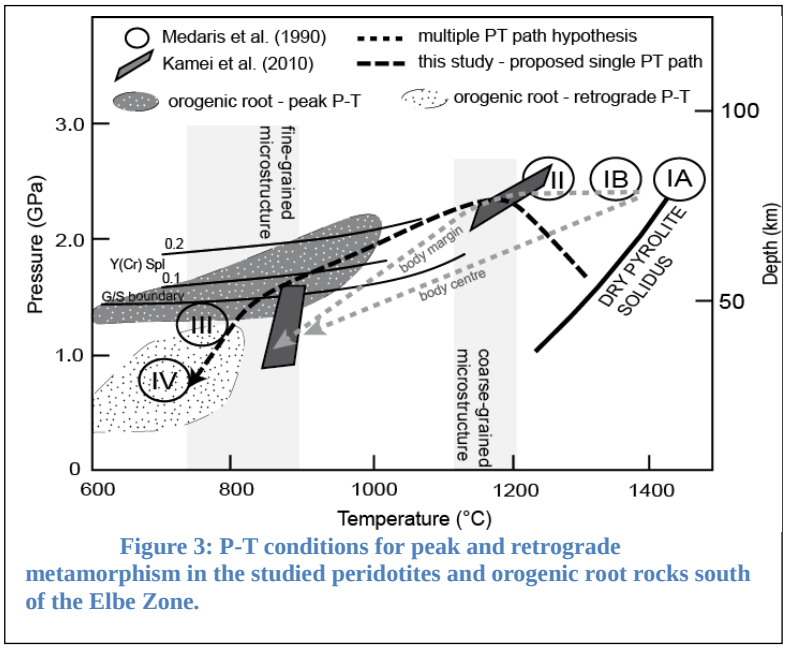

Figure 3: P-T conditions for peak and retrograde metamorphism in the studied peridotites and orogenic root rocks south of the Elbe Zone.

Site 1: Granulites

Four deformation fabrics have been recognized within the NGM directly surrounding the Mohelno peridotite body. Both S1 and S2 fabrics contain a granulite facies mineral assemblage such as garnet, kyanite, perthitic feldspar and rutile. Rare original coarse-grained granulite S1 fabric occurs in low-strain domain within the internal part of the peridotite fold hinge and is defined by either weak mineral aggregate alignment or lithological layering. Reworking of the

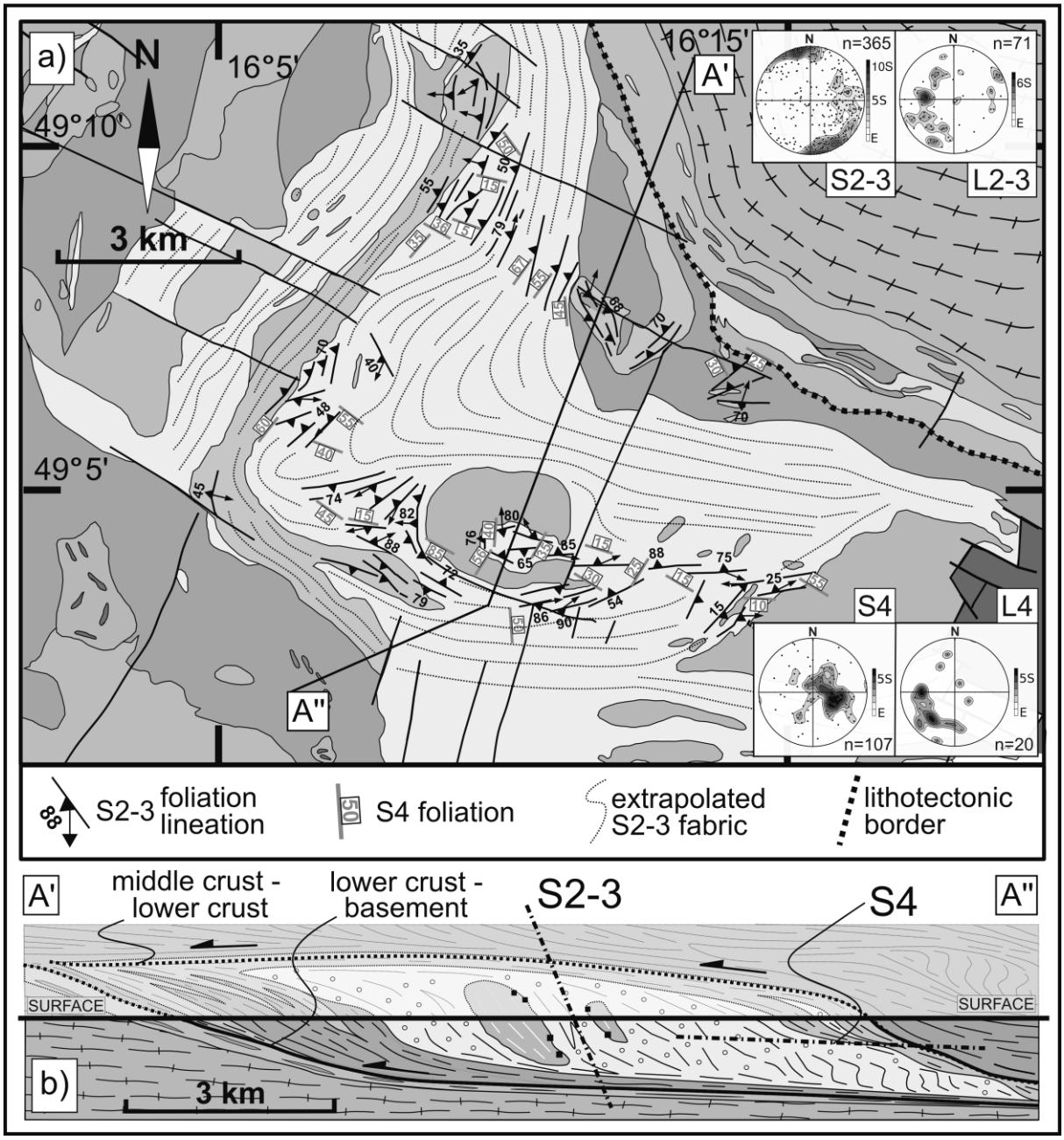

Figure 4: Structures in granulites observed in the field: a) the structural map of the studied area shows trajectories of S2 foliation, contoured pole figures of mylonitic fine-grained foliations (S2) and lineations (L2) in granulites as well as S3 and L3 structures; b) the cross-section shows a Náměšť granulite massif as a low strain domain preserving steep S2-3 mylonitic foliations affected by S4 flat fabric due to underthrusting of Brunia basement promontory.

S1 fabric is associated with development of (ultra)mylonitic granulite S2 fabric associated with development of isoclinal fold F2 (Fig. 5b). S2 foliation is striking N-S in the north and E-W in the south (Fig. 4a). Close to MPB the E-W trending S2 is always steep and follows the trend of peridotite fold, and bear mineral lineation moderately plunging to the west (Fig. 4a). The granulite along limbs of MPB fold is locally retrogressed in amphibolite facies conditions resulting in formation of highly elongated lenses of a granitic melt forming composite S2-3 foliation with relictual granulite facies fabric. Large scale fold is accompanied with meter scale parasitic F3 folds. Granulites with such an S3 microstructure has been also observed along shear zones cross-cutting internal margin of peridotite fold (Fig. 5c). This retrograde S3 fabric is defined by the shape-preferred orientation of amphibolites

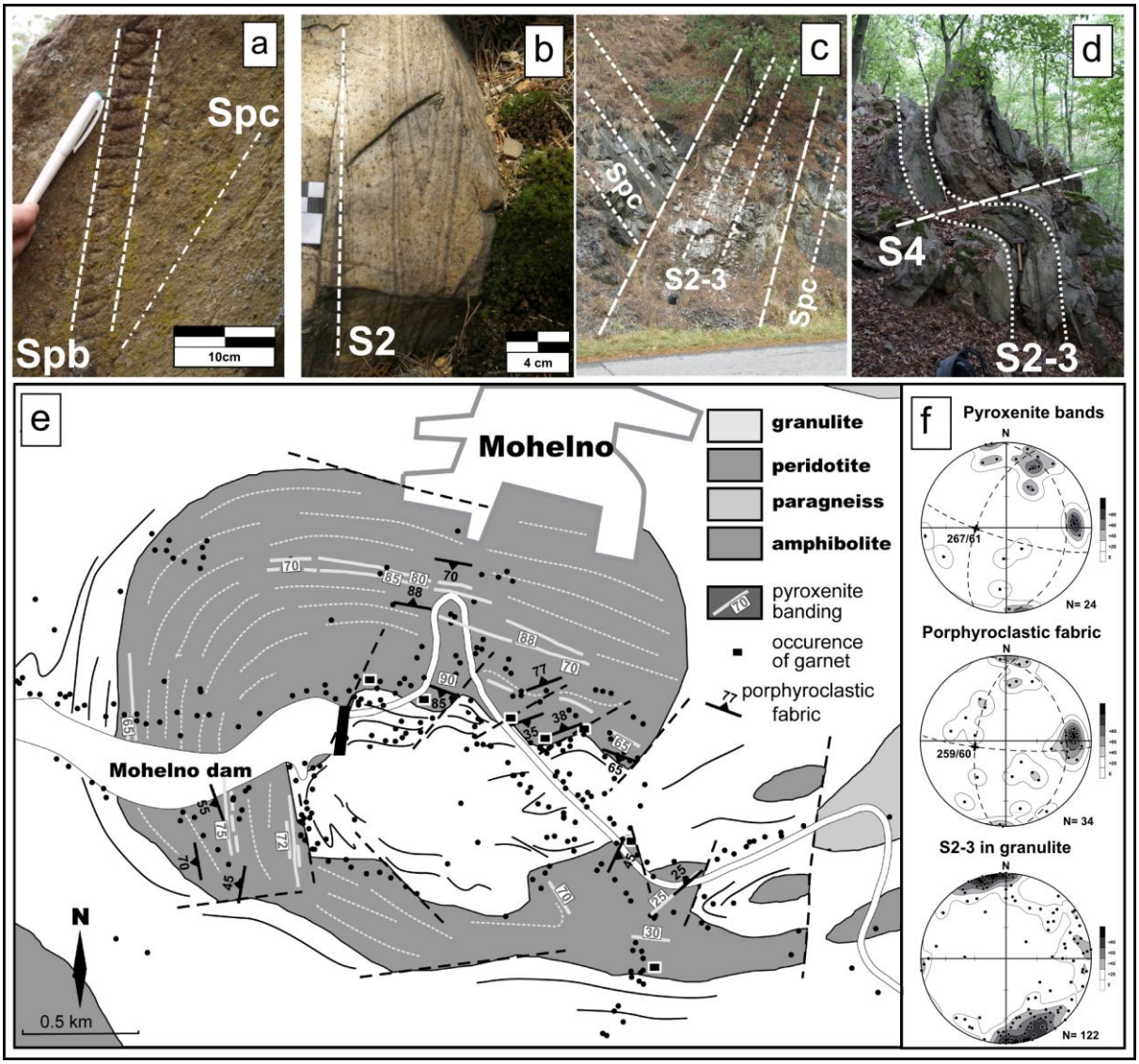

Figure 5: Main structural elements in the close vicinity of the Mohelno peridotite body defined in the field. a) Mylonitic foliation in peridotite is defined by elongated porphyroclasts of orthopyroxenes and rework also websterite layers that occur parallel or oblique to the mylonitic foliation; b) mylonitic fine-grained foliation S2 in granulites show often isoclinal folds; c) a granulite-peridotite interface along the inner fold with felsic partial melts and granulite wedging towards the peridotite; d) localized flat S3 shear zones in granulites rework suvbertical S2 foliation; e) a simplified geological map of the studied area shows trajectories of the mylonitic foliation and websterite layering in peridotites and S2 foliation in granulites. Occurrences of garnet (black squares) and sampling sites (black circles) are shown as well as foliations measured in the field; f) contoured pole figures of the poles to porphyroclastic foliation, websterite layers and S2 together with S3 foliations.

facies mineral assemblage such as sillimanite and biotite and by layers and lenses of granitic melt.

The retrogressed granulites reworked by subhorizontal S4 foliation are widespread in the NGM. The D4 deformation exhibits different degree of S2-3 fabric transposition according to orientation of S2-3 mechanical anisotropy. In the volumetrically more important western part of the NGM, the N-S and E-W striking steep S2-3 foliation is reworked by flat shear zones and recumbent open folds with N-S and E-W trending hinges, respectively (Fig. 5d). In the eastern extremity of the massif the degree of the D4 deformation is more important leading to development of close to isoclinal E-W trending F4 folds associated with development of pervasive S4 migmatitic foliation. Here, the S4 is marked by preferred orientation of biotite and coarse leucosome layers. The S4 bears SW plunging mineral and

stretching lineation marked by alignment of sillimanite and elongation of quartz-feldspar aggregates.

Sites 2, 3 and 4: Peridotites

A structural pattern of the Mohelno peridotite reveals rather homogeneous mylonitic fabric and pyroxenite layering while surrounding granulite and amphibolite exhibit polyphase structural evolution (Fig. 5). A special attention has been paid to a distribution of garnet and coarse spinel within the Mohelno Peridotite Body (MPB). Our study shows that a spinel variety occupies the majority of the peridotite body, while the garnet is rimming the internal margin of the fold hinge with exception of one sample located in the southeastern extremity of the peridotite body (Site 2, Fig. 5e). In general, the peridotite mineral assemblage is rarely preserved thanks to extensive serpentinization. Both coarse-grained spinel and garnet bearing peridotite is mylonitized resulting in development of fine-grained spinel bearing matrix and orthopyroxene porphyroclasts (Fig. 5a). This mylonitic foliation is generally steeply dipping and its orientation follows the fold shape of the peridotite body with the fold hinge steeply plunging to the west (Sites 2, 3 and 4, Fig. 5e). The second fabric element is represented by milimetres to several centimetres thick bands of websterites to orthopyroxenites (Site 4, Fig. 5a) that form layers either parallel or oblique with respect to principal mylonitic fabric. Pyroxenite layers are also mylonitized and affected by late fractures which progressively disappear in surrounding serpentinized matrix. Exceptionally, a late penetration of partially molten granulite to peridotite along a cleavage plane can be observed at the internal granulite-

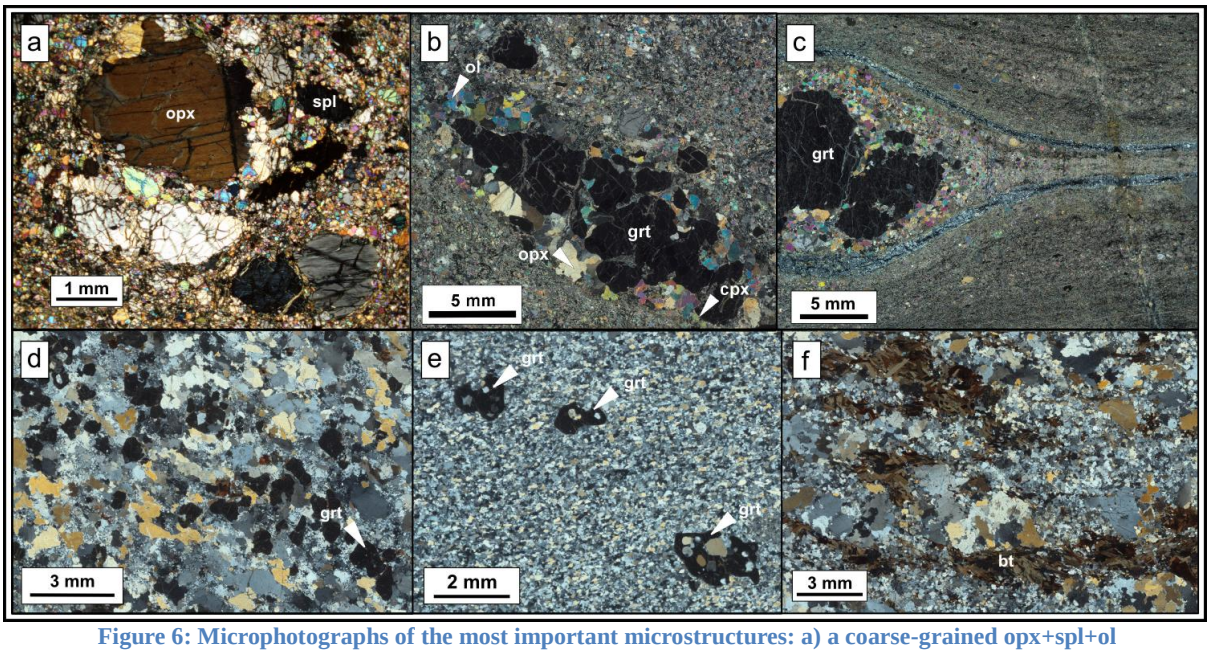

Figure 6: Microphotographs of the most important microstructures: a) a coarse-grained opx+spl+ol porphyroclastic domain characterise the original mineral association in the majority of the peridotite body; b) elongated garnet replace spinel in coarse-grained microstructure along the inner margin of the body; c) garnet-pyroxene porphyroclast surrounded by serpentinized mylonitic microstructure; d) coarse S1 microstructure in granulite, with core-mantle features; e) ultra-mylonitic S2 microstructure; f) S3microstructure in granulite.

peridotite interface (Site 3).

Internal strain fabric inferred from a measurement of lattice preferred orientation of olivine and orthopyroxene

The goal of the LPO measurements was to determine active slip systems of olivine

and orthopyroxene and to interpret resulting patterns. These informations are used to deduce: a) orientation of main fabric elements preserved from serpentinization using eigenvector and eigenvalue classification. Both analyses as well as projection of pole figures have been carried out by software from the shareware package (ftp://www.gm.univ-montp2.fr/mainprice//CareWare_Unicef_Programs/); b) deformation regime (Tommasi et al., 1999); c) temperature (Demouchy et al., 2009; Tommasi et al., 2000) and d) water content (Chopra and Paterson, 1984; Jung and Karato, 2001; Mackwell et al., 1985).

Lattice preferred orientation of olivine is not uniform in the measured samples. The eigenvalue classification showed a strong component of random distribution in all samples, but also distinguished two types of LPO patterns (Fig. 7). The first type shows girdle distribution of the [100] axes with the sub-maximum inside the girdle and broad point maximum of the normals to (010) planes providing the strongest maximum. The [001] axes

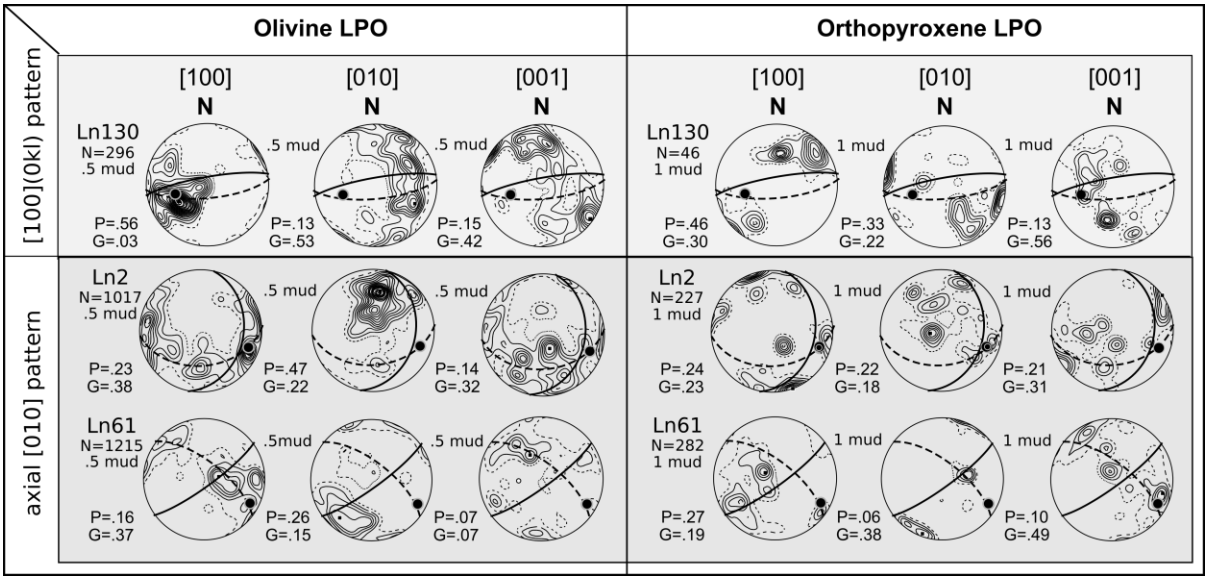

Figure 7: LPO of olivine and orthopyroxene show parallelism of the olivine [100] with opx [001] maxima positions which represent independent control of the stretching lineation determination. Pole figures are in equal area projection and lower hemisphere, and contoured at interval 0.5 and 1.0 times of uniform distribution in olivine and opx, respectively. N is a number of measured grains and P, G and R values are calculated from the eigenvalue analysis.

show generally weak preferred orientation, but some samples show a weak point maximum (Fig. 7). In the Vollmer's diagram the [100] axis plot in between G and R corners, indicating girdle dominated distribution of this axis, while the [010] plot between P and R apexes suggesting more point type distribution (Fig. 8b). This LPO is characteristic for the AG-type (Mainprice, 2007) or axial [010] pattern according to Tommasi et al. (2000). It is developed preferentially along the inner margin of the fold-shaped peridotite body. Locally, it has been also measured in a few samples from the central part of the southern limb of MPB fold (Fig. 8a). The second LPO type shows the strongest point maximum of [100] and girdle distribution for both the [010] and the weakest [001] axes (Fig. 7). In the Vollmer's diagram the [100] axes plot between P and R corners while the [010] axes plot in between G and R apexes. Such a type of texture corresponds to [100](0kl) pattern (Tommasi et al., 2000) or D-type (Jung and Karato, 2001; Karato et al., 1980; Mainprice, 2007) and is typically developed in the interior and along the outer parts of the fold shape peridotite body (Fig. 8a). Both LPO patterns imply that studied peridotites have been deformed at high stress and 'dry' conditions (Jung and Karato, 2001; Karato et al., 1980; Mainprice, 2007).

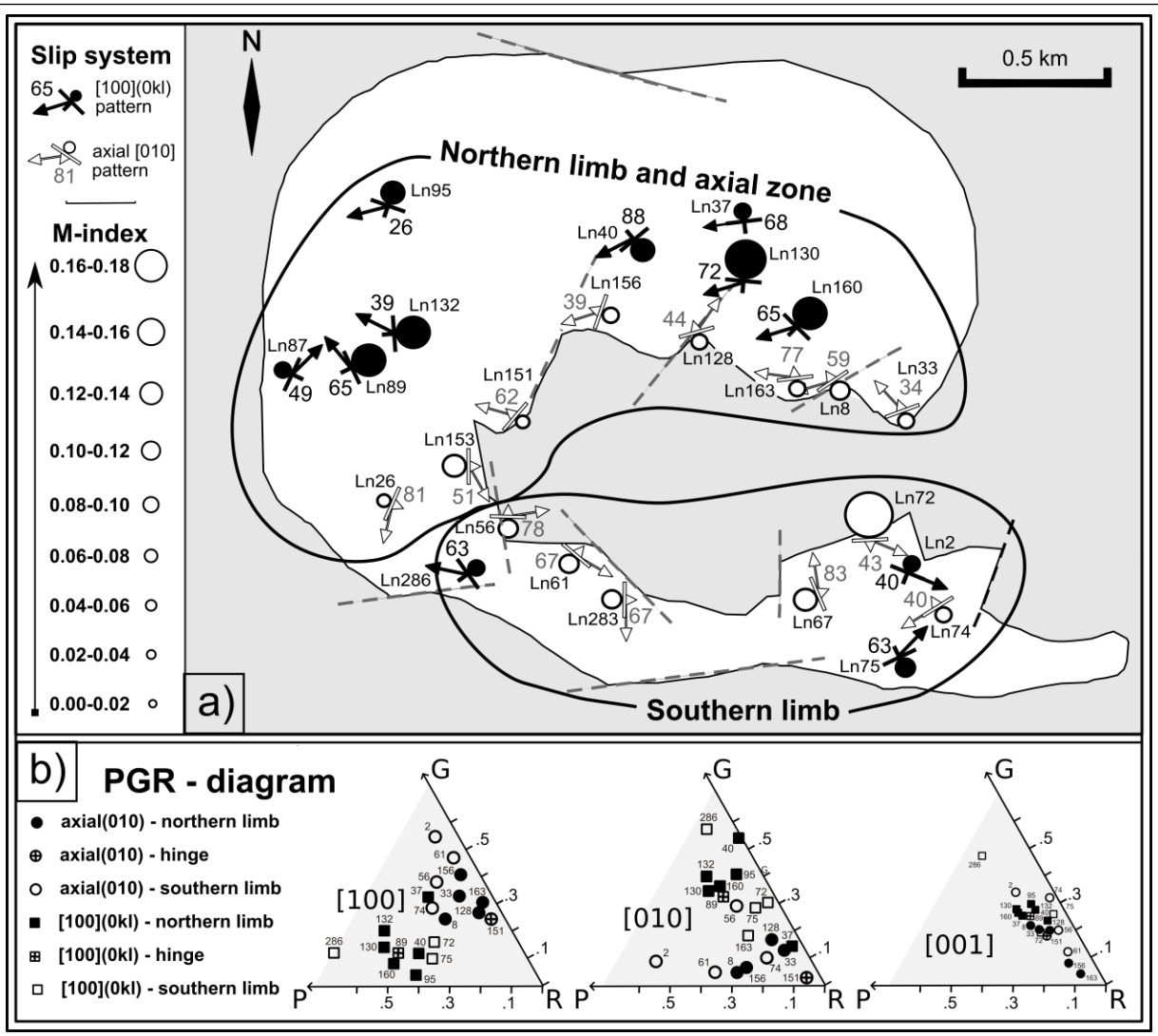

Figure 8: A) Orientations of foliation and lineation within the Mohelno serpentinized peridotite body according to the eigenvector analysis of olivine LPO. LPO revealed that the axial [010] pattern occur mainly along the inner margin and the southern limb of the fold, while the [100](0kl) pattern occur in the rest of the body. Strength of LPO represented by values of M-index for each measured sample are presented in the map with contours of the MPB; b) point-girdle-random (PGR) diagrams for main crystallographic directions. Each symbol in individual diagram represents one measured sample. Round symbol (spots) characterizes LPO with [100](010) or axial [010] pattern either along the inner margin (black spots) or inside (white spots) the body. Square symbol corresponds to the [100](0kl) pattern.

In several sites the macroscopic lineation or both lineation and foliation were not known and therefore the eigenvector analysis was used to identify the orientation of these fabric elements. Because, the [100](010) slip system is the most active in both LPO types the maximum eigenvector orientations for the [100] and [010] axes have been attributed to the stretching lineation and the pole of foliation, respectively. In order to confirm the orientation of lineation and foliation deduced from olivine LPO the lattice preferred orientation of orthopyroxene was measured in several samples.

Relationship between field structure and olivine LPO

Field observations carried out in the Náměšť granulite body show well preserved S2 steep mylonitic fabric concordant with olivine and opx foliation of the fold-shaped Mohelno Peridotite Body (Fig. 5). In order to compare internal strain pattern of the peridotite with surrounding granulite, the orientations of the constructed olivine foliations and lineations were projected in the map (Fig. 8a) and into the stereographic projections (Fig. 9). The

structural map shows that the olivine foliations generally follow the shape of the peridotite body for both types of LPO. The axial [010] type distribution is dominant along the inner margin of the body and along the southern limb of the large fold thereby coinciding only partly with occurrence of garnet. In contrast, the axial [100] pattern is developed in the

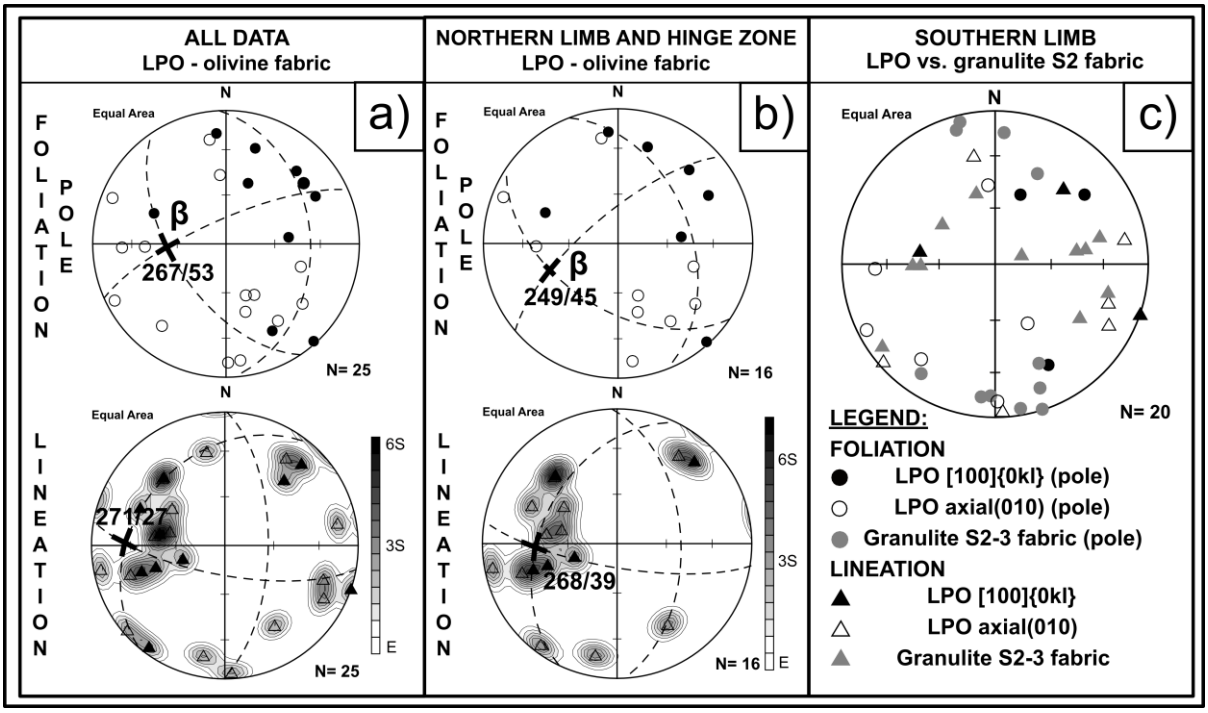

Figure 9: Lower hemisphere, equal area stereographic projections of poles to foliations and lineations calculated from a) all olivine LPO data; b) LPO data from the fold northern limb and the hinge zone; c) LPO data from the fold southern limb and adjacent granulite.

northern limb and the hinge of the MPB fold.

The poles to foliation of all LPO data (Fig. 9a) are dominantly distributed along a great circle and the pole of the great circle coincides with the megafold hinge (β-axis of Sander (1930), Fig. 5). In addition, the lineations obtained from [100](0kl) pattern occupy a similar position in stereographic diagram (Fig. 9a). In contrast, lineations from the axial[010] are rotated along the fold hinge. This fabric pattern can be interpreted as a result of large scale folding of pre-existing olivine fabric and its rotation around fold hinge. Our data show that the high M-index coincides with prolate fabric in the hinge and northern limb of the MPB fold compared to oblate fabric and weak M index in the southern limb and inner part of the northern limb. This pattern can be explained by two phase structural evolution. During the first stage the whole peridotite body acquired weak oblate deformation related to emplacement of mantle sheet into lower crustal granulites (Fig. 10b). Subsequently, the vertical N-S striking sheet becomes folded due to horizontal N-S shortening and vertical extrusion (Fig. 11c) as proposed by Franěk et al. (2011); Lexa et al. (2011). The vertical extrusion is associated with folding of peridotite sheet and favors constrictional deformation in fold hinges, while folded limbs can preserve oblate fabrics. If the form of vertical extrusion channel has circular or elliptical section, the constrictional flow is producing folds with vertical hinges due to lateral shortening of vertical anisotropy (Kratinová et al., 2006; Weijermars, 1993).

Thermal and mechanical interactions of mantle and crust

Medaris et al. (2005) proposed that the Mohelno peridotite corresponds to the depleted upper mantle which originated during Late Devonian intracontinental rifting. This is the period when originated the early spinel preserved in garnet porphyroblasts (Medaris et al., 1990). This lithosphere thinning was replaced by crustal thickening and development of orogenic root 70 km thick (Schulmann et al., 2009; Schulmann et al., 2005). The crustal thickening model fits well with petrological studies of spinel and garnet peridotites which reveal that both coarse-grained microstructure equilibrated at similar temperatures 1100-1200°C at pressures of around 2.3GPa (Fig.10; (Kamei et al., 2010; Medaris et al., 1990). Such PT values could be regarded as peak PT conditions of Mohelno peridotite and mineral zoning may reflects position of spinel-garnet isograde in the mantle. In such a setting the spinel – garnet transition is located only 5 – 10 km underneath the double thickened Moho corresponding to depth of 80 km (Fig. 10a). Rheology of the lithosphere for both thinning and thickening stages was calculated according to Thompson et al. (2001) and Schulmann et al. (2002) and indicates that the warm and thin mantle lithosphere was inherited from the thinning stage. This tectonic setting is supposed to be necessary prerequisite for further

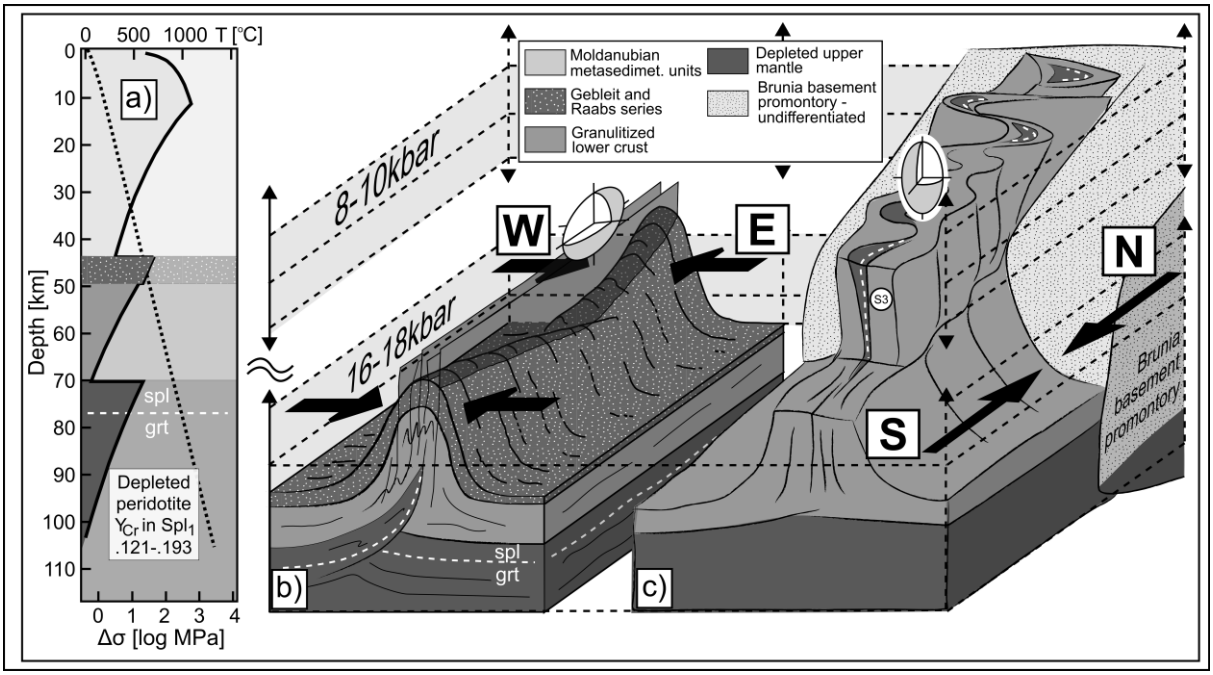

Figure 10: Tectonic evolution of the Mohelno peridotite body: a) rheological profile through thickened orogenic crust with indicated primary microstructures of peridotite and granulite shown in circles, b) 3D model of imbrications of mantle lithosphere and emplacement of peridotite sheet into folded lower crust during the stage D2. Oblate ellispsoid is shown indicating development of first crystal plastic deformation in the cooled peridotite. c) Model of indentation of Brunia promontory orthogonal to S2 fabrics and development of F3 folds with steep fold hinges affecting both peridotite and granulite. Prolate ellipsoid is shown for fold hinge deformation.

tectonic evolution (Fig. 10a).

Tectonic evolution continues by mylonitization of peridotites and enclosed pyroxenite layers that could be linked to the process of development of intramantle shear zone followed by imbrications of peridotite and granulite at the bottom of orogenic root during ongoing E-W shortening (Fig. 10b). This shortening event is responsible for the formation of N-S trending crustal megafolds and gravity driven overturns transporting lower crustal and mantle fragments upwards (Lexa et al., 2011; Schulmann et al., 2009; Schulmann et al., 2008)). The conditions of mantle shearing during emplacement into crust are recorded in clinopyroxene-spinel II kelyphite assemblage around garnets, which may be correlated to kyanite, K-feldspar and garnet assemblage in surrounding granulites (Kamei et al., 2010; Medaris et al.,

2005; Medaris et al., 1990). Progressively, both peridotite and granulite assemblages equilibrated at temperatures and pressures of 800-900°C and 1.5-0.8GPa (Fig. 10).

Field structural observations as well as EBSD study show that S2 fabric in granulites and porphyroclastic fabric in peridotites were actively folded during large scale F3 folding of the MPB during partial melting of granulite and D3 amphibolite facies retrogression. This event is correlated to the development of amphibole-spinel coronas around garnet estimated to 700°C and 0.5-0.8GPa (Fig. 3; stage IV of Medaris et al. (1990)). A similar transition from granulite fine-grained mylonitic fabric (S2) to coarser-grained fabric (S3) associated to partial melting has been described in other granulites in the Bohemian Massif as a result of decompression after rapid ascent of hot granulites to the mid-crustal levels (Franěk et al., 2006; Franěk et al., 2011). The F3 folding occurred in the regional scale and is associated with indentation of thickened orogenic root by the Brunian promontory (Fig. 10c) as proposed by Schulmann et al. (2008). According to these authors, the S4 fabric records the later subhorizontal channel flow which transported passively the peridotite and granulite fold in partially molten rocks above the Brunia basement.

Emplacement of the Mohelno peridotite body along the high-stress shear zone into the granulite followed by ascent to the mid-crustal levels and active folding fits well also to bilinear cooling histories calculated from composition of garnets. Medaris et al. (1990) showed that the garnet core temperatures in excess of 1100°C required extremely rapid cooling to quench the low almandine composition in the garnet interior. This event reflects emplacement of hot peridotite into the colder granulitic lower crust during early stages of D2 event. The existence of garnet rim zoning requires a significant decrease of the cooling rate during isothermal decompression associated with vertical ascent of granulite and peridotites to the mid crustal levels during late stages of D2 and D3.

References

Carswell, D. A., O'Brien, P. J., (1993). Thermobarometry and Geotectonic Significance of High-Pressure Granulites: Examples from the Moldanubian Zone of the Bohemian Massif in Lower Austria. J. Petrol. 34, 427-459.

Chopra, P. N., Paterson, M. S., (1984). The role of water in the deformation of dunite. J. Geophys. Res. 89(B9), 7861-7876.

Cooke, R. A., (2000). High-pressure/temperature metamorphism in the St. Leonhard Granulite Massif, Austria: evidence from intermediate pyroxene-bearing granulites. Int. J. Earth Sci. 89, 631-651.

Cooke, R. A., O'Brien, P. J., (2001). Resolving the relationship between high P-T rocks and gneisses in collisional terranes: an example from the Gföhl gneiss-granulite association in the Moldanubian Zone, Austria. Lithos 58, 33-54.

Demouchy, S., Schneider, S. E., Mackwell, S. J., Zimmerman, M. E., Kohlstedt, D. L., (2009). Experimental deformation of olivine single crystals at lithospheric temperatures. Geophys. Res. Lett. 36, L04304.

Dobretsov, N., Mísař, Z., Popov, E., (1984). The P-T conditions of equilibrium for some pyrope peridotite and country rocks in the Moldanubian area at Mohelno (Eastern Moravia, Czechoslovakia). Miner. Slov. 16, 87-95..

Edel, J., Weber, K., (1995). Cadomian terranes, wrench faulting and thrusting in the central Europe Variscides: geophysical and geological evidence. Geol. Rundsch. 84, 412-432.

Fiala, J., Matějovská, O., Vaňková, V., (1987). Moldanubian granulites and related rocks:petrology, geochemistry and radioactivity. Rozpr. Česk. Akad. Věd, Řada Mat. Přír. Věd 97, 1-102.

Franke, W., (2000). The mid-European segment of the Variscides: tectonostratigraphic units, terrane boundaries and plate tectonic evolution, in: Franke, W., Haak, V., Oncken, O., D., T. (Eds.), Orogenic Processes: Quantification and Modelling in the Variscan Belt. Geological Society, London, Special Publications 179, pp. 35-61.

Franěk, J., Schulmann, K., Lexa, O., (2006). Kinematic and rheological model of exhumation of high pressure granulites in the Variscan orogenic root: example of the Blanský les granulite, Bohemian Massif, Czech Republic. Mineral. Petrol. 86, 253-276.

Franěk, J., Schulmann, K., Lexa, O., Tomek, Č., Edel, J.-B., (2011). Model of syn-convergent extrusion of orogenic lower crust in the core of the Variscan belt: implications for exhumation of high-pressure rocks in large hot orogens. J. Metamorph. Geol. , in press.

Hasalová, P., Janoušek, V., Schulmann, K., Štípská, P., Erban, V., (2008a). From orthogneiss to migmatite: Geochemical assessment of the melt infiltration model in the Gföhl Unit (Moldanubian Zone, Bohemian Massif). Lithos 102, 508-537.

Hasalová, P., Schulmann, K., Lexa, O., Štípská, P., Hrouda, F., Ulrich, S., Haloda, J., Týcová, P., (2008b). Origin of migmatites by deformation-enhanced melt infiltration of orthogneiss: a new model based on quantitative microstructural analysis. J. Metamorph. Geol. 26, 29-53.

Janoušek, V., Finger, F., Roberts, M., Frýda, J., Pin, C., Dolejš, D., (2004). Deciphering the petrogenesis of deeply buried granites: whole-rock geochemical constraints on the origin of largely undepleted felsic granulites from the Moldanubian Zone of the Bohemian Massif. Earth Env. Sci. T. R. So. 95, 141-159.

Janoušek, V., Holub, F. V., (2007). The causal link between HP-HT metamorphism and ultrapotassic magmatism in collisional orogens: case study from the Moldanubian Zone of the Bohemian Massif. P. Geologist. Assoc. 118, 75-86.

Jung, H., Karato, S.-i., (2001). Water-Induced Fabric Transitions in Olivine. Science 293, 1460-1463.

Kamei, A., Obata, M., Michibayashi, K., Hirajima, T., Svojtka, M., (2010). Two Contrasting Fabric Patterns of Olivine Observed in Garnet and Spinel Peridotite from a Mantle-derived Ultramafic Mass Enclosed in Felsic Granulite, the Moldanubian Zone, Czech Republic. J. Petrol. 51, 101-123.

Karato, S.-I., Toriumi, M., Fujii, T., (1980). Dynamic recrystallization of olivine single crystals during high-temperature creep. Geophys. Res. Lett. 7, 649-652.

Kratinová, Z., Závada, P., Hrouda, F., Schulmann, K., (2006). Non-scaled analogue modelling of AMS development during viscous flow: A simulation on diapir-like structures. Tectonophysics 418, 51-61.

Lexa, O., Schulmann, K., Janoušek, V., Štípská, P., Guy, A., Racek, M., (2011). Heat sources and trigger mechanisms of exhumation of HP granulites in Variscan orogenic root. J. Metamorph. Geol. 29, in press.

Mackwell, S. J., Kohlstedt, D. L., Paterson, M. S., (1985). The Role of Water in the Deformation of Olivine Single Crystals. J. Geophys. Res. 90(B13), 319-333.

Mainprice, D., (2007). Seismic anisotropy of the deep Earth from a mineral and rock physics perspective, in: Schubert, G. (Eds.), Treatise on Geophysics vol. 2. Elsevier Ltd., pp. 437-492.

Matějovská, O., (1975). The Moldanubian gneiss series of south-western Moravia and its relation to granulites.. Věstn. Ústřed. Ústav. Geol. 50, 345-351.

Medaris, L. J., Wang, H., Jelínek, E., Mihaljevič, M., Jakeš, P., (2005). Characteristics and origins of diverse Variscan peridotites in the Gföhl Nappe, Bohemian Massif, Czech Republic. Lithos 82, 1-23.

Medaris, L. J., Wang, H., Mísař, Z., Jelínek, E., (1990). Thermobarometry, diffusion modelling and cooling rates of crustal garnet peridotites: Two examples from the

Moldanubian zone of the Bohemian Massif. Lithos 25, 189-202.
Racek, M., Štípská, P., Pitra, P., Schulmann, K., Lexa, O., (2006). Metamorphic record of burial and exhumation of orogenic lower and middle crust: a new tectonothermal model for the Drosendorf window (Bohemian Massif, Austria). Mineral. Petrol. 86, 221-251.
Racek, M., Štípská, P., Powell, R., (2008). Garnet-clinopyroxene intermediate granulites in the St. Leonhard massif of the Bohemian Massif: ultrahigh-temperature metamorphism at high pressure or not?. J. Metamorph. Geol. 26, 253-271.
Sander, B., 1930. Gefügekunde der Gesteine, Vienna: Springer, .
Schulmann, K., Konopásek, J., Janoušek, V., Lexa, O., Lardeaux, J.-M., Edel, J.-B., Štípská, P., Ulrich, S., (2009). An Andean type Palaeozoic convergence in the Bohemian Massif. C. R. Geosci. 341, 266-286.
Schulmann, K., Kroner, A., Hegner, E., Wendt, I., Konopásek, J., Lexa, O., Štípská, P., (2005). Chronological constraints on the pre-orogenic history, burial and exhumation of deep-seated rocks along the eastern margin of the Variscan Orogen, Bohemian Massif, Czech Republic. Am. J. Sci. 305, 407-448.
Schulmann, K., Martelat, J.-E., Ulrich, S., Lexa, O., Štípská, P., Becker, J. K., (2008). Evolution of microstructure and melt topology in partially molten granitic mylonite: Implications for rheology of felsic middle crust. J. Geophys. Res. 113, B10406.
Schulmann, K., Schaltegger, U., Ježek, J., Thompson, A. B., Edel, J.-B., (2002). Rapid burial and exhumation during orogeny: Thickening and synconvergent exhumation of thermally weakened and thinned crust (Variscan orogen in Western Europe). Am. J. Sci. 302, 856-879.
Tajčmanová, L., Konopásek, J., Schulmann, K., (2006). Thermal evolution of the orogenic lower crust during exhumation within a thickened Moldanubian root of the Variscan belt of Central Europe. J. Metamorph. Geol. 24, 119.
Thompson, A., Schulmann, K., Ježek, J., Tolar, V., (2001). Thermally softened continental extensional zones (arcs and rifts) as precursors to thickened orogenic belts. Tectonophysics 332, 115-141.
Tollmann, A., (1982). Grossräumiger variszischer Deckenbau im Moldanubikum und neue Gedanken zum Variszikum Europas. Geotekton. Forsch. 64, 1-91.
Tommasi, A., Mainprice, D., Canova, G., Chastel, Y., (2000). Viscoplastic self-consistent and equilibrium-based modeling of olivine lattice preferred orientations: Implications for the upper mantle seismic anisotropy. J. Geophys. Res. 105, 7893-7908.
Tommasi, A., Tikoff, B., Vauchez, A., (1999). Upper mantle tectonics: three-dimensional deformation, olivine crystallographic fabrics and seismic properties. Earth Planet. Sci. Lett. 168, 173 - 186.
Urban, M., (1992). Kinematics of the Variscan thrusting in the Eastern Moldanubicum (Bohemian Massif, Czechoslovakia): evidence from the Náměšt granulite massif. Tectonophysics 201, 371-391.
Weijermars, R., (1993). Progressive deformation of single layers under constantly oriented boundary stresses. J. Struct. Geol. 15, 911-922.
Šichtařová, I., (1981). Moldanubian amphibolites in the area SE of Náměšt nad Oslavou. Věstn. Ústřed. Ústav. Geol. 56, 203-214.
Štípská, P., Schulmann, K., Kroner, A., (2004). Vertical extrusion and middle crustal spreading of omphacite granulite: a model of syn-convergent exhumation (Bohemian Massif, Czech Republic). J. Metamorph. Geol. 22, 179-198.
Štípská, P., Schulmann, K., Powell, R., (2008). Contrasting metamorphic histories of lenses of high-pressure rocks and host migmatites with a flat orogenic fabric (Bohemian Massif, Czech Republic): a result of tectonic mixing within horizontal crustal flow?. J. Metamorph. Geol. 26, 623-646.